



## Discover Generics

Cost-Effective CT & MRI Contrast Agents



WATCH VIDEO

# AJNR

## Neuroimaging in Pediatric Patients with Juvenile Xanthogranuloma of the CNS

B.L. Serrallach, S.F. Kralik, B.H. Tran, T.A.G.M. Huisman, R.P. Patel, C.E. Allen, K.L. McClain, N. Gulati, C.Q. Dillard-Ilboudo, M.J. Hicks, C.A. Mohila and N.K. Desai













This information is current as of June 3, 2025.

*AJNR Am J Neuroradiol* 2022, 43 (11) 1667-1673

doi: <https://doi.org/10.3174/ajnr.A7683>

<http://www.ajnr.org/content/43/11/1667>

# Neuroimaging in Pediatric Patients with Juvenile Xanthogranuloma of the CNS

 B.L. Serrallach,  S.F. Kralik,  B.H. Tran,  T.A.G.M. Huisman,  R.P. Patel,  C.E. Allen,  K.L. McClain,  N. Gulati,  C.Q. Dillard-Ilboudo,  M.J. Hicks,  C.A. Mohila, and  N.K. Desai



## ABSTRACT

**BACKGROUND AND PURPOSE:** Juvenile xanthogranuloma is a rare clonal, myeloid, neoplastic disorder. Typically, juvenile xanthogranuloma is a self-limited disorder of infancy, often presenting as a solitary red-brown or yellow skin papule/nodule. A small subset of patients present with extracutaneous, systemic juvenile xanthogranuloma, which may include the CNS. The goal of this retrospective study was to evaluate and categorize the neuroimaging findings in a representative cohort of pediatric patients with CNS juvenile xanthogranuloma.

**MATERIALS AND METHODS:** The brain and/or spine MR imaging data of 14 pediatric patients with pathology-proven juvenile xanthogranuloma were categorized and evaluated for the location; the signal intensity of xanthogranulomas on T1WI, T2WI, DWI, and a matching ADC map for the pattern and degree of contrast enhancement; and the presence of perilesional edema, cysts, or necrosis.

**RESULTS:** Fourteen pediatric patients (8 girls, 6 boys; mean age, 84 months) were included in the study. Patients presented with a wide variety of different symptoms, including headache, seizure, ataxia, strabismus, hearing loss, facial paresis, and diabetes insipidus. Juvenile xanthogranuloma lesions were identified in a number of different sites, including supra- and infratentorial as well as intracranial and spinal leptomeningeal. Five patients were categorized into the neuroradiologic pattern unifocal CNS juvenile xanthogranuloma; 8, into multifocal CNS juvenile xanthogranuloma; and 1, into multifocal CNS juvenile xanthogranuloma with intracranial and spinal leptomeningeal disease. In most cases, xanthogranulomas were small-to-medium intra-axial masses with isointense signal on T1WI (compared with cortical GM), iso- or hyperintense signal on T2WI, had restricted diffusion and perilesional edema. Almost all xanthogranulomas showed avid contrast enhancement. However, we also identified less common patterns with large lesions, nonenhancing lesions, or leptomeningeal disease. Four cases had an additional CT available. On CT, all xanthogranulomas were homogeneously hyperdense (solid component) without evident calcifications.

**CONCLUSIONS:** CNS juvenile xanthogranuloma may demonstrate heterogeneous neuroimaging appearances potentially mimicking other diseases, such as primary brain neoplasms, metastatic disease, lymphoma and leukemia, other histiocytic disorders, infections, or granulomatous diseases.

**ABBREVIATIONS:** ALK = anaplastic lymphoma kinase; BRAF V600 = B-Raf proto-oncogene, serine/threonine kinase (V600E); CE = contrast-enhanced; ECD = Erdheim-Chester disease; GRE = gradient recalled-echo; HLH = hemophagocytic lymphohistiocytosis; JXG = juvenile xanthogranuloma; LCH = Langerhans cell histiocytosis; MAPK = mitogen-activated protein kinase; RDD = Rosai-Dorfman disease

Juvenile xanthogranuloma (JXG) is a rare, clonal, myeloid, neoplastic disorder traditionally belonging to the group of non-

Langerhans cell histiocytosis.<sup>1,2</sup> Typically, JXG is a self-limited condition in infancy with skin lesions often presenting as a solitary red-brown or yellow skin papule or nodule on the head, neck, or upper trunk.<sup>3,4</sup> A small subset present with systemic JXG, which is commonly progressive without therapy and is potentially fatal.<sup>2,5</sup> Extracutaneous systemic involvement may include the eyes, oral cavity, heart, lung, gastrointestinal tract, liver, spleen, kidneys, lymph nodes, bone marrow, soft tissue, and the CNS.<sup>5-7</sup> Characteristic histopathologic features include vacuolated CD163, factor-XIIIa- and fascin-positive histiocytic cells, and multinucleated Touton giant cells (which may not be present in CNS lesions).<sup>5,8</sup> Involvement of the CNS is seen in only up to 7% of cases with JXG.<sup>5,9</sup> The clinical

Received May 31, 2022; accepted after revision August 8.

From the Edward B. Singleton Department of Radiology (B.L.S., S.F.K., B.H.T., T.A.G.M.H., R.P.P., N.K.D.), Department of Pediatrics (C.E.A., K.L.M., N.G., C.Q.D.-I.), Section of Hematology-Oncology, and Department of Pathology and Immunology (M.J.H., C.A.M.), Texas Children's Hospital and Baylor College of Medicine, Houston, Texas.

B.L. Serrallach was supported by the Edward B. Singleton endowment.

Please address correspondence to Bettina L. Serrallach, MD, Edward B. Singleton Department of Radiology, Texas Children's Hospital and Baylor College of Medicine, 6701 Fannin St, Suite 470, Houston, TX 77030; e-mail: bettinaserallach@icloud.com



Indicates article with online supplemental data.

<http://dx.doi.org/10.3174/ajnr.A7683>

presentation of CNS JXG is nonspecific and includes a wide range of symptoms, such as headache, seizures, ataxia, increased intracranial pressure, macrocrania, developmental delay, weakness, numbness, cranial nerve abnormalities, and diabetes insipidus.<sup>1,2,5,10</sup> To date, there is no generally accepted consensus or standard-of-care treatment for CNS JXG. Successful outcomes have been reported in individual cases and case series, including chemotherapy (eg, clofarabine), anaplastic lymphoma kinase (*ALK*) inhibition (for *ALK* fusion events), or mitogen-activated protein kinase (*MAPK*) pathway blockade with B-Raf proto-oncogene, serine/threonine kinase (V600E) (*BRAF* V600E) or mitogen-activated protein kinase kinase (*MAP2K*) inhibitors.<sup>5,11,12</sup> Only scarce literature on imaging in CNS JXG exists, and the imaging spectrum remains incompletely characterized.<sup>1,6,7,13-15</sup> Accordingly, the goal of this article was to study and categorize the neuroimaging findings in a representative cohort of pediatric patients with confirmed CNS JXG.

## MATERIALS AND METHODS

Following institutional review board approval, an electronic search of the pediatric histopathologic and pediatric neuroradiologic database covering January 1, 2010, to August 31, 2021, was performed using the following keywords: juvenile xanthogranuloma (JXG). Inclusion criteria for this retrospective study were the following: 1) pediatric patients (younger than 19 years of age) with pathology-proven JXG (from CNS and/or other lesions), and 2) brain and/or spine MR imaging data (indication: initial diagnostic work-up of newly emerged symptoms).

All MR imaging studies were performed at either 1.5T or 3T magnetic field strength. Images were obtained by different institutions, but protocols mostly included axial and/or sagittal T1WI and axial T2WI, axial FLAIR, axial contrast-enhanced T1-weighted (T1+CE) images, axial SWI or T2\*-gradient recalled-echo (T2\*-GRE) sequences, and axial DWI or DTI. Isotropic diffusion-weighted images were generated; and matching ADC maps were automatically calculated using vendor-specific software. The relevant clinical and histopathologic data, including the age at diagnosis/biopsy, age at initial imaging, sex, sites of disease involvement, presenting symptoms, histologic diagnosis, and clinical molecular data were extracted from the electronic medical charts.

MR imaging studies were independently reviewed and categorized on the PACS workstation by 2 board-certified pediatric neuroradiologists (N.K.D. and R.P.P.). The readers were not blinded to the patient's medical history. The interrater reliability was assessed by the Cohen  $\kappa$  (for categoric variables) and the intraclass correlation coefficient (for interval and metric variables). The MR imaging studies were evaluated for the exact location (including an intra- versus extra-axial classification), the T1WI and T2WI signal intensity of xanthogranulomas (hypo-, iso-, or hyperintense compared with the cortical GM), the pattern of contrast enhancement (contrast enhancement versus no contrast enhancement; homogeneous contrast enhancement versus heterogeneous contrast enhancement), the degree of contrast enhancement (none, mild, moderate, marked), the percentage (proportion of the mass; visually estimated) of contrast enhancement of the lesion (0%–25%, 26%–50%, 51%–75%, and 76%–100%), the extent of perilesional T2-weighted hyperintensity suggestive of vasogenic

edema (no, mild, moderate, marked), evidence of blood products or calcium on SWI or T2\*-GRE (yes/no), the presence of cysts or necrosis (yes/no; "cyst" was defined as a well-defined collection, and "necrosis", as a nonsolid irregular area), and the signal intensity on DWI and the matching ADC map (diffusion restriction or no diffusion restriction with reference to the brain). In addition, quantitative measurements of ADC values were performed. An ROI was manually placed within the xanthogranuloma on the ADC maps as follows: section with the largest expansion of the solid component of the xanthogranuloma using a 5-mm<sup>2</sup> ROI. The mean ADC value and the standard deviation (SD) were determined.

Statistical analyses were performed using the software package SPSS Statistics, Version 28.0 (IBM).

## RESULTS

Fourteen pediatric patients (8 girls, 6 boys; mean age, 84 months at imaging; median age, 65.5 months; age range, 1 month to 18 years 11 months) fulfilled the inclusion criteria. Patients were categorized into 3 primary neuroradiologic patterns: 1) unifocal, 2) multifocal, and 3) multifocal leptomeningeal. Five subjects had unifocal CNS JXG (Fig 1 and Online Supplemental Data), 8 patients had multifocal CNS JXG (Fig 2), and 1 child had multifocal CNS JXG with additional intracranial and spinal leptomeningeal disease (Fig 3).

Isolated CNS involvement was found in all 5 patients categorized into the unifocal neuroradiologic pattern. Of the 8 patients categorized into the multifocal neuroradiologic pattern, 2 had a single-system involvement of the CNS, while 6 patients showed involvement of  $\geq 2$  organ systems. From the latter, the skin was involved in all 6 patients, followed by bone involvement in 3 patients. Furthermore, 1 patient had, in addition to CNS and skin involvement, lesions in the conjunctiva and eye globe; 1 patient had, in addition to CNS and skin involvement, a lesion in the soft tissue (pharynx); and 1 patient had extensive systemic involvement with lesions in the CNS, skin, bone, lung, kidneys, and lymph nodes. The 1 patient categorized into the multifocal leptomeningeal neuroradiologic pattern had lesions in the CNS and peripheral nervous system. In total, 7 of 14 patients (50%) had isolated CNS involvement, and 7 patients (50%) had involvement of  $\geq 2$  organ systems. The involved organ systems of all 14 patients are summarized in the Online Supplemental Data.

Xanthogranulomas had an average maximum diameter at presentation of 2.2 (SD, 1.3) cm (range, 0.8–4.8 cm). Lesions were found in a number of different sites, including supra- and infratentorial, intra-axial or extra-axial (in the hypothalamic-pituitary region, the internal auditory canal, or the Meckel cave), as well as in spinal leptomeningeal locations. With the 5 subjects categorized into the neuroradiologic pattern, unifocal CNS JXG, lesions were located in the right frontal lobe (cortical/subcortical WM; Fig 1), in the left parietal lobe (cortical/subcortical WM; Online Supplemental Data), cerebellar vermis, pons, and infundibulum. With patients with multifocal CNS JXG, lesions were scattered supra- and infratentorially (Figs 2 and 3). Supratentorial lesions were mainly found in the cortex, subcortical WM, or central GM, followed by deep WM and periventricular WM. Infratentorial xanthogranulomas were located in the pons in 6 patients; in the

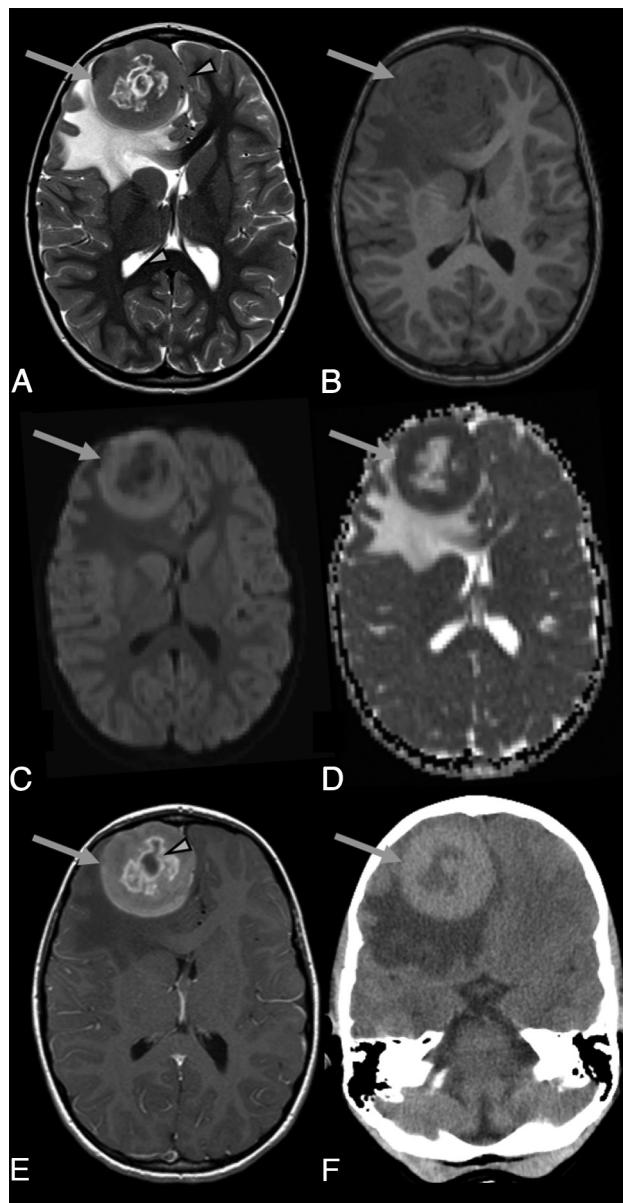


**FIG 1.** Brain images of a 6-year-old girl with pathology-proven unifocal JXG who presented with increased frequency of headaches, occasionally accompanied by vomiting. Brain MR imaging with an axial T2-weighted image (A), axial T1-weighted image (B), axial DWI (C), axial ADC map (D), axial T1+CE-weighted image (E), and axial noncontrast CT (F) shows a large, round, unifocal mass lesion located in the right frontal lobe (arrows in A–F) with central necrosis (arrowhead in E), perilesional edema, and right-to-left midline shift (arrowhead in A). Compared with cortical GM, the solid non-necrotic peripheral component of the lesion is T2-isointense (A) and T1-isointense (B) and shows contrast enhancement (E) and restricted diffusion (C and D). The axial CT image (F) demonstrates the hyperdense (solid portion), large mass lesion.

cerebellar GM in 5 patients; in the brachium pontis in 3 patients; in the cerebellar WM in 2 patients; in the midbrain in 2 patients; in the vermis in 1 patient; and in the medulla in 1 patient. Lesions were found in the infundibulum in 6 patients; in the corpus callosum, pituitary gland, and hypothalamus in 3 patients each; in the optic chiasm and septum pellucidum in 2 patients each; in

the ventricles in 1 patient; and in the internal auditory canal and the Meckel cave on both sides in 1 patient. In 1 patient, the infundibulum was involved in isolation, and in 5 patients, the infundibulum was part of a multifocal manifestation. Two children were diagnosed with diabetes insipidus. In 1 patient, diabetes insipidus was an initial presenting symptom, and the other patient developed diabetes insipidus later in the disease course.

Images were obtained from different institutions. In 2 patients, no T1WI (12/14 with available T1WI); in 1 child, no T2WI (13/14 with available T2WI); in 4 subjects, no DWI (10/14 with available DWI); and in 3 patients no SWI/T2\*-GRE (11/14 with available SWI/T2\*-GRE) images were available. On T1WI, xanthogranulomas were isointense compared with cortical GM in 7 patients (7/12), hyperintense in 4 patients (4/12), and hypo- to isointense in 1 patient (1/12). In the 12 patients with available T1WI, the pituitary bright spot was lost in 3 subjects (3/12). The infundibulum was involved in all 3 patients in whom the pituitary bright spot was lost. On T2WI, xanthogranulomas were isointense compared with cortical GM in 5 patients (5/13), hyperintense in 4 patients (4/13), iso- to hyperintense in 3 patients (3/13), and hypo- to isointense in 1 patient (1/13), respectively. In 13 patients with available T2WI, perilesional edema was evident in 11 patients (11/13). The xanthogranulomas of 2 patients had no edema, and 4 patients had mild, 3 patients had moderate, and 4 patients had marked perilesional edema. Necrosis was seen in 6 patients (6/14), and 2 patients (2/14) had cystic components within the lesions. The xanthogranulomas of 13 patients (13/14) showed contrast enhancement on T1+CE-weighted images; the xanthogranulomas of 6 patients had homogeneous and the xanthogranulomas of 5 patients had heterogeneous contrast enhancement. In 2 patients with multifocal JXG, larger xanthogranulomas showed heterogeneous and smaller xanthogranulomas showed homogeneous contrast enhancement. One patient with multifocal xanthogranulomas had lesions with and without contrast enhancement on T1+CE-weighted images. All contrast-enhancing xanthogranulomas were characterized by marked contrast enhancement, comprising >50% of the lesion size, with 13 patients having 76%–100%, and 1 patient having 51%–75% of the lesion enhancing.

Seven of 10 patients with available DWI (7/10) showed restricted diffusion, and 3 had no restricted diffusion (equivalent values compared with normal brain on the ADC map; increased ADC values were not found). The mean ADC values and SD were determined on the available ADC maps. For 1 patient, no measurement could be obtained because the small size of the lesion prevented proper ROI positioning. The overall ( $n = 9$ ) mean ADC value was 868.96 (SD, 179.24); the mean ADC value calculated for lesions with diffusion restriction ( $n = 7$ ) was 823.97 (SD, 175.99); and without diffusion restriction ( $n = 2$ ), it was 1026.42 (SD, 86.15).

Three of 11 patients with available SWI or T2\*-GRE images demonstrated hypointense blood products or calcifications.

Due to an obstructive mass effect of the xanthogranulomas, hydrocephalus was found in 2 patients (2/14).

In 9 patients (9/14), additional spine MRIs were available. By means of these spine MRIs, spinal leptomeningeal disease



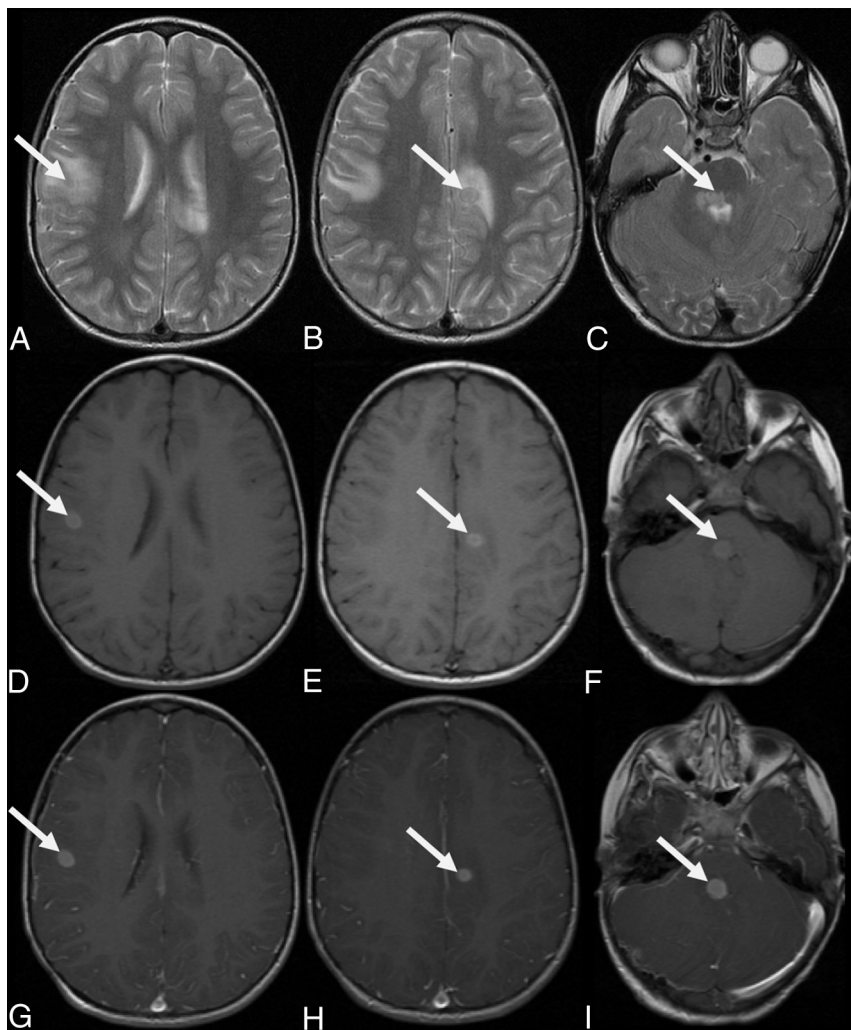


**FIG 2.** Brain MR images of a 3-year-old boy with pathology-proven multifocal JXG and new-onset strabismus. Axial T2-weighted (A–C), axial T1-weighted (D–F), and axial T1+CE-weighted (G–I) MR imaging sequences show exemplary 3 round-to-oval lesions located in the right (arrows in A, D, and G) and left paracentral (arrows in B, E, and H) regions and the pons (arrows in C, F, and I), respectively. Compared with cortical GM, the lesions are T2-iso- to hyperintense (A–C) and T1-hyperintense (D–F) and show homogeneous contrast enhancement (G–I) and mild perilesional edema.

was found in 1 patient (neuroradiologic pattern: multifocal leptomeningeal).

In addition to MRIs, 4 patients had an additional CT available. Xanthogranulomas were homogeneously hyperdense (solid component) on all 4 CT scans without evident calcifications. Two demonstrated central necrosis; and 1, a marginal cyst.

The interrater reliability was assessed using the Cohen  $\kappa$  (for categorical variables) and by the intraclass correlation coefficient (for interval and metric variables). The Cohen  $\kappa$  and the intraclass correlation coefficient values ranged from 0.71 to 1.00. According to Field,<sup>16</sup> values of  $>0.7$  represent reliable ratings.

Detailed information comprising the demographics, imaging features, and clinical information including the clinical mutational data are shown as Online Supplemental Data. A summary focusing on the signal characteristics of CNS xanthogranulomas is presented in the Table.

## DISCUSSION

In this cohort of pediatric patients with biopsy-proven CNS JXG (from the CNS site and/or from other locations), most JXG lesions were typified by small-to-medium masses with iso-intense signal on T1WI, iso- or hyper-intense signal on T2WI, restricted diffusion and perilesional edema. Almost all xanthogranulomas showed marked contrast enhancement. Cases were categorized into 3 primary neuroradiologic patterns: unifocal, multifocal, and multifocal leptomeningeal.

The category of histiocytosis includes Langerhans cell histiocytosis (LCH), Erdheim-Chester disease (ECD), JXG, Rosai-Dorfman disease (RDD), hemophagocytic lymphohistiocytosis (HLH), and malignant histiocytosis. These entities are characterized by pathogenic myeloid cells that share histologic features with macrophages or dendritic cells.<sup>5,8</sup> The lesional cells may originate from the embryonic yolk sac, fetal liver, or postnatal bone marrow.<sup>5</sup> The term “histiocytic disorders” for LCH, ECD, JXG, RDD, and HLH has been proposed to differentiate them from hyperproliferative cancer-typical lesions such as Langerhans cell sarcoma and malignant histiocytosis.<sup>5</sup> While LCH, ECD, JXG, and RDD have somatic mutations in *MAPK* pathway genes and show an accumulation of clonal, mononuclear phagocytes, HLH is a syndrome of immune dysregulation.<sup>5,8</sup>

The Working Group of the Histiocyte Society published the first classification system of histiocytic diseases in 1987, which consisted of 3 categories, namely,

Langerhans cell histiocytosis, histiocytosis of mononuclear phagocytes other than Langerhans cells, and malignant histiocytic disorders.<sup>17</sup> In the past decades with the incorporation of molecular features, there have been several revisions, with the most recent revision in 2016.<sup>8,18</sup> This updated contemporary classification consists of 5 groups (the Langerhans-related; cutaneous and mucocutaneous histiocytoses; malignant histiocytoses; RDD; and HLH and macrophage activation syndrome) and is based on histology, phenotype, molecular alterations, and clinical characteristics.<sup>8</sup> The proposed Langerhans group includes LCH, ECD, and extracutaneous JXG.<sup>8</sup>

Depending on the histiocytic entity, these diseases may be seen in both the pediatric and adult populations in various proportions and may show a broad variety of clinical presentations and outcomes.<sup>1,5,8,18</sup> The intense inflammatory infiltrates in histiocytic disorders play a key role in the origination and maintenance of

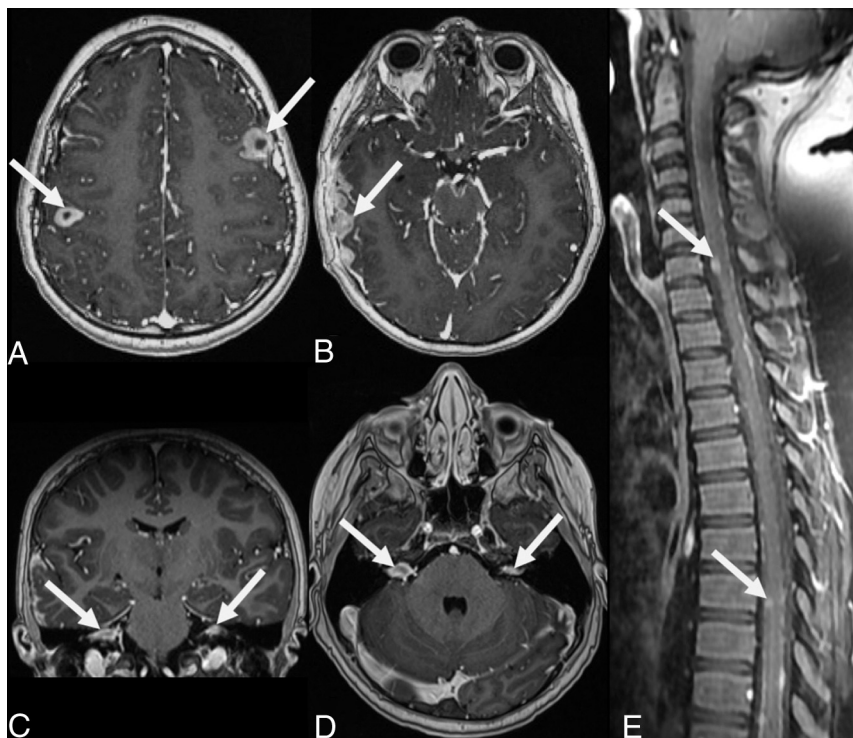


**FIG 3.** MR images obtained in a 10-year-old boy with pathology-proven multifocal JXG with leptomeningeal brain and spine involvement. The patient presented with progressive right-ear pain and erythema and decreased hearing and right-sided facial nerve palsy along with headaches. Axial (A, B, and D) and coronal T1+CE-weighted (C) MR images of the brain. E, Sagittal T1+CE-weighted fat-suppressed MR image of the spine. For example, 2 centrally necrotic, peripherally contrast-enhancing lesions are noted within both cerebral hemispheres (arrows in A). In addition, nodular contrast enhancement involving the leptomeninges of the right temporal lobe (arrow in B) and contrast enhancement within both internal auditory canals (arrows in C and D) are shown. Sagittal T1+CE-weighted images of the spine depict increased contrast enhancement of the leptomeninges (“sugar coating”), partially with nodular components, most obvious at the C7 and T8 level (arrows in E).

organ-specific lesions and contribute to the clinical symptoms.<sup>5</sup> To date, very little is known concerning the underlying pathogenetic mechanisms of JXG.<sup>5</sup> JXG cells share some common features with dermal macrophages, including expression of fascin, factor-XIIIa, CD163, and CD68 (Online Supplemental Data).<sup>5</sup>

JXG is a rare entity; a frequency of approximately 1 per million children and a male/female ratio of 1.4:1 have been described in the Kiel Pediatric Tumor Registry.<sup>9</sup> In our cohort, there was a 1.33:1 female predominance. With systemic JXG, a predominance of females of up to 3:1 has been reported in the literature.<sup>19</sup> Most often, JXG presents in children (< 4 years) as a solitary red-brown or yellow skin papule or nodule of 0.5–1 cm in diameter and may undergo spontaneous regression.<sup>2,3,5,8</sup> Most skin lesions involve the head, neck, or upper trunk.<sup>3,4</sup> Some patients have isolated or very few cutaneous lesions, while others may develop hundreds of lesions.<sup>5</sup> A small subset present with systemic JXG.<sup>2</sup> Besides the CNS (7%), extracutaneous JXG may involve the liver (22%), lungs (16%), soft tissue (16%), spleen (11%), eyes (9%), oral cavity (7%), adrenal glands (7%), gastrointestinal tract (7%), lymph nodes (7%), bone marrow (7%), and heart (4%).<sup>5–7</sup> In this study, 7 of 14 patients (50%) had isolated CNS involvement. Seven patients (50%) had involvement of  $\geq 2$  organ systems, with involvement of

the skin and/or bones being most common (Online Supplemental Data).

The clinical presentation depends on the involved organ systems.<sup>5,10</sup> For CNS JXG, clinical presentation is nonspecific and includes headache, seizures, ataxia, increased intracranial pressure, macrocrania, developmental delay, weakness, numbness, cranial nerve abnormalities, and diabetes insipidus.<sup>1,2,5,10</sup> These findings are in line with the initial presentation of the patients in our study, which included headache, seizure, ataxia, strabismus, hearing loss, facial palsy, and diabetes insipidus, among others (Online Supplemental Data).

In general, JXG is a self-limiting disease.<sup>4</sup> However, systemic JXG, especially with CNS involvement, may be associated with long-term problems such as structural damage by brain lesions or liver failure by large hepatic tumors or may even be fatal.<sup>2,5,9,20</sup> Available treatment options for JXG include “wait and see/follow-up,” chemotherapy (eg, clofarabine), targeted therapies such as *ALK* inhibition (for *ALK* fusion events) and *MAPK* pathway blockade with *BRAF* V600E or *MAP2K* inhibitors, surgery, or a combination of these modalities.<sup>5,9,11,12,14</sup> Most skin-limited JXG lesions show spontaneous involution, but surgical excision may be considered if lesions are cosmetically unacceptable or endanger or impair

functions such as vision or swallowing.<sup>5</sup> In patients with systemic JXG including CNS lesions, there is evidence of successful treatment using chemotherapy (eg, clofarabine) or targeted therapies such as *MAPK* pathway blockade, or *ALK* inhibition (for *ALK* fusion events).<sup>5,11,12</sup>

Recurrent activating somatic mutations in *MAPK* genes have been identified in JXG.<sup>5,8</sup> In our cohort, there were 1 patient with coexisting LCH and JXG and 1 patient with coexisting JXG and RDD. There is evidence of the coexistence of JXG and LCH<sup>21</sup> and JXG and RDD,<sup>22</sup> supporting a potential common cell of origin.<sup>5</sup> Additionally, JXG has been reported in patients with neurofibromatosis 1 and other “RASopathies”.<sup>23,24</sup> JXG can be found in up to 29% of patients with neurofibromatosis 1,<sup>24</sup> consistent with the known role of *MAPK* pathway activation in the pathogenesis of both diseases.<sup>25</sup> The literature concerning a triple association between JXG, neurofibromatosis 1, and juvenile myelomonocytic leukemia is contradictory, with some studies suggesting an association<sup>26</sup> and others reporting no increased incidence.<sup>24</sup> In addition, there is a rare subtype of histiocytic disorder, the *ALK*-positive histiocytosis, which is mainly associated with *KIF5B-ALK* fusions and shows frequent neurologic involvement and may have a successful outcome with *ALK* inhibition treatment.<sup>12</sup> A subgroup of *ALK*-

**Imaging features of CNS JXG<sup>a</sup>**

No.	T1-Weighted	T2-Weighted	T1+CE	DWI/ADC
4/12	↔	↔	4 Marked contrast enhancement	4 Diffusion restriction
3/12	↔	↔ - ↑ or ↑	3 Marked contrast enhancement	1 Diffusion restriction, 2 no diffusion restriction
2/12	↑	↑	2 Marked contrast enhancement	1 Diffusion restriction, 1 NA
2/12	↑	↔ or ↔ - ↑	1 Marked contrast enhancement/1 with lesions with marked and lesions without contrast enhancement	1 No diffusion restriction, 1 NA
1/12	↓ - ↔	↓ - ↔	1 Marked contrast enhancement	1 Diffusion restriction

**Note:** ↔ indicates isointense; ↑, hyperintense; ↔ - ↑, iso- to hyperintense; ↓ - ↔, hypo- to isointense; NA, not applicable.

<sup>a</sup> Cases were included only when both T1WI and T2WI were available.

positive histiocytosis demonstrates histopathologic features of classic JXG.<sup>12</sup> Additionally, recurrent mutations in *CSF1R* have recently been described in JXG.<sup>27</sup>

To date, data describing imaging features of CNS JXG are largely limited to case studies<sup>1,6,13-15</sup> and reviews, including clinical and pathological aspects as well as a summary description of the imaging features.<sup>2</sup> This article aims to present a large case series focusing on neuroimaging features of CNS JXG in children. Intracranial xanthogranulomas have been described variously as T1-/T2-hypo-, iso-, or hyperintense lesions on MR imaging.<sup>1,2,6,13-15,20</sup> In our cohort, on T1WI, xanthogranulomas were mainly isointense compared with cortical GM (7/12; Online Supplemental Data), several lesions were hyperintense (4/12; Fig 2), and 1 lesion was hypo- to isointense (1/12). On T2WI, xanthogranulomas were mainly isointense (5/13; Fig 1 and Online Supplemental Data) or hyperintense (4/13), followed by an iso- to hyperintense (3/13; Fig 2) or hypo- to isointense (1/13) appearance.

Ginat et al<sup>28</sup> characterized the imaging features of head and neck xanthogranulomas of 10 patients, with 6 patients undergoing MR imaging.<sup>28</sup> They reported that on T1WI, lesions were characterized by an iso- or hyperintensity, and on T2WI, by an iso- or hypointensity.<sup>28</sup> Within our cohort, several lesions showed a high signal on T1WI and T2WI. This could be due to lipid components within these lesions because lipidized or xanthomatous cells may be found within xanthogranulomas.<sup>29</sup> In general, CNS JXGs<sup>1,2</sup> and head and neck JXGs<sup>28</sup> are described as showing homogeneous contrast enhancement on T1+CE-weighted images. Marked contrast enhancement seems to be a reliable imaging feature of JXG because almost all xanthogranulomas showed avid contrast enhancement (Fig 1–3 and Online Supplemental Data), and only 1 patient (1/14) who had multifocal xanthogranulomas showed lesions with marked contrast enhancement as well as lesions without contrast enhancement on T1+CE-weighted images. Most lesions (7/10) demonstrated restricted diffusion (Figs 1 and Online Supplemental Data). This finding is in agreement with the literature describing decreased diffusion in such lesions.<sup>1,28</sup> Ginat et al described decreased diffusivity as likely attributed to hypercellularity and/or a collagenous matrix.

Because there are heterogeneous, non-pathognomonic imaging appearances of CNS JXG with neuroradiologic patterns ranging from unifocal to multifocal leptomeningeal involvement, neuroradiology alone is not able to provide an accurate diagnosis. Accordingly, a wide array of differential diagnoses must be considered, including primary brain neoplasms, lymphoma and leukemia, other histiocytic disorders such as LCH or ECD, and infections. If multifocal lesions with leptomeningeal involvement are evident, metastatic and granulomatous diseases such as sarcoidosis and tuberculosis should be included in the differential diagnosis.

The range of intracranial CNS findings in LCH is better known and com-

prises a neurodegenerative pattern including infratentorial WM abnormalities more pronounced in the peridentate regions, abnormalities of the dentate nuclei and basal ganglia, and bilateral symmetric leukoencephalopathy-like abnormalities in the supratentorial white matter.<sup>30-32</sup> In addition, CNS LCH may show mass lesions in the hypothalamic-pituitary region, seen as thickening and enhancement of the pituitary stalk with possibly loss of the posterior bright spot, and it is clinically frequently accompanied by diabetes insipidus.<sup>31,32</sup> Rare neuroimaging manifestations include enlargement of the pineal gland, thickening and enhancement of the choroid plexus, and intraparenchymal masses.<sup>31,32</sup> Hence, in contrast to CNS JXG, in CNS LCH, intra-axial parenchymal mass lesions are rather uncommon. However, involvement of the hypothalamic-pituitary region appears to be a common feature of both CNS JXG and LCH. In our cohort, infundibular involvement was seen in 6 patients, and pituitary gland or hypothalamic involvement was noted in 3 patients each. In addition, the posterior pituitary gland T1-hyperintense signal or bright spot was absent in 3 patients. In general, a loss of the posterior bright spot is thought to be a result of a lack of vasopressin-containing granules.<sup>31</sup> We assume a similar mechanism as seen in LCH, in which an absent pituitary bright spot and involvement of the infundibulum are frequent but do not necessarily occur in all patients. In our cohort, we did not find changes suggestive of posterior fossa neurodegeneration. In addition to CNS LCH, neurodegeneration has also been described in the context of ECD.<sup>33</sup> CNS JXG may not be prone to neurodegeneration, or neurodegeneration could potentially develop later in the course of the disease because neuroimaging in our cohort was performed for the initial diagnostic work-up of new symptoms.

We are aware of several limitations in our study. The imaging findings are based on a retrospective study design with a quite limited number of pediatric patients and MR imaging was performed as a diagnostic work-up of newly emerged symptoms on various scanners with somewhat different protocols. Subsequent studies with larger cohorts and standardized imaging protocols are needed to confirm the proposed imaging patterns presented in our study. In addition, future prospective studies should correlate histologic features to neuroimaging characteristics, and longitudinal follow-up



studies may shed more light on the rate of progression, the response to therapy, and the possible changes in imaging characteristics.

## CONCLUSIONS

In this study, pediatric patients with biopsy-proven CNS JXG were categorized into 3 primary neuroradiologic patterns: 1) unifocal, 2) multifocal, and 3) multifocal leptomeningeal. CNS JXG lesions were typified by small-to-medium masses with isointense signal on T1WI, iso- or hyperintense signal on T2WI, restricted diffusion, perilesional edema, and marked contrast enhancement. However, we also identified less common patterns with large lesions, nonenhancing lesions, or leptomeningeal disease. These findings demonstrate the heterogeneous neuroimaging appearances of JXG potentially mimicking other diseases, such as primary brain neoplasms, metastatic disease, lymphoma and leukemia, other histiocytic disorders, and infections or granulomatous diseases. Pediatric neuroradiologists should be familiar with this entity.

## ACKNOWLEDGMENT

The authors thank M. Christiner for providing statistical support.

**Disclosure forms** provided by the authors are available with the full text and PDF of this article at [www.ajnr.org](http://www.ajnr.org).

## REFERENCES

- Deisch JK, Patel R, Koral K, et al. **Juvenile xanthogranulomas of the nervous system: a report of two cases and review of the literature.** *Neuropathology* 2013;33:39–46 [CrossRef Medline](#)
- Wang B, Jin H, Zhao Y, et al. **The clinical diagnosis and management options for intracranial juvenile xanthogranuloma in children: based on four cases and another 39 patients in the literature.** *Acta Neurochir (Wien)* 2016;158:1289–97 [CrossRef Medline](#)
- Hock M, Zelger B, Schweigmann G, et al. **The various clinical spectra of juvenile xanthogranuloma: imaging for two case reports and review of the literature.** *BMC Pediatr* 2019;19:128 [CrossRef Medline](#)
- Szczerkowska-Dobosz A, Kozicka D, Purzycka-Bohdan D, et al. **Juvenile xanthogranuloma: a rare benign histiocytic disorder.** *Postepy Dermatol Alergol* 2014;31:197–200 [CrossRef Medline](#)
- McClain KL, Bigenwald C, Collin M, et al. **Histiocytic disorders.** *Nat Rev Dis Primers* 2021;7:73 [CrossRef Medline](#)
- Meshkini A, Shahzadi S, Zali A, et al. **Systemic juvenile xanthogranuloma with multiple central nervous system lesions.** *J Cancer Res Ther* 2012;8:311–13 [CrossRef Medline](#)
- Rajendra B, Duncan A, Parslew R, et al. **Successful treatment of central nervous system juvenile xanthogranulomatosis with cladribine.** *Pediatr Blood Cancer* 2009;52:413–45 [CrossRef Medline](#)
- Emile JF, Ablan O, Fraïtag S, al; Histiocyte Society. **Revised classification of histiocytoses and neoplasms of the macrophage-dendritic cell lineages.** *Blood* 2016;127:2672–81 [CrossRef Medline](#)
- Janssen D, Harms D. **Juvenile xanthogranuloma in childhood and adolescence: a clinicopathologic study of 129 patients from the Kiel Pediatric Tumor Registry.** *Am J Surg Pathol* 2005;29:21–28 [CrossRef Medline](#)
- Freyer DR, Kennedy R, Bostrom BC, et al. **Juvenile xanthogranuloma: forms of systemic disease and their clinical implications.** *J Pediatr* 1996;129:227–37 [CrossRef Medline](#)
- Diamond EL, Durham BH, Ulaner GA, et al. **Efficacy of MEK inhibition in patients with histiocytic neoplasms.** *Nature* 2019;567:521–24 [CrossRef Medline](#)
- Kemps PG, Picarsic J, Durham BH, et al. **ALK-positive histiocytosis: a new clinicopathologic spectrum highlighting neurologic involvement and responses to ALK inhibition.** *Blood* 2022;139:256–80 [CrossRef Medline](#)
- Ernemann U, Skalej M, Hermisson M, et al. **Primary cerebral non-Langerhans cell histiocytosis: MRI and differential diagnosis.** *Neuroradiology* 2002;44:759–63 [CrossRef Medline](#)
- Gressot LV, Patel AJ, Bollo RJ, et al. **Disseminated intracranial juvenile xanthogranulomatosis in a neonate without cutaneous lesions.** *J Neurosurg Pediatr* 2013;12:187–91 [CrossRef Medline](#)
- Orsey A, Paessler M, Lange BJ, et al. **Central nervous system juvenile xanthogranuloma with malignant transformation.** *Pediatr Blood Cancer* 2008;50:927–30 [CrossRef Medline](#)
- Field AP. *Discovering Statistics Using SPSS (Introducing Statistical Methods)*. 3rd ed. SAGE Edge; 2009
- Writing Group of the Histiocyte Society. **Histiocytosis syndromes in children.** *Lancet* 1987;1:208–09 [Medline](#)
- Favara BE, Feller AC, Pauli M, et al. **Contemporary classification of histiocytic disorders: the WHO Committee on Histiocytic/Reticulum Cell Proliferations—Reclassification Working Group of the Histiocyte Society.** *Med Pediatr Oncol* 1997;29:157–66 [CrossRef Medline](#)
- Isaacs H Jr. **Fetal and neonatal histiocytoses.** *Pediatr Blood Cancer* 2006;47:123–29 [CrossRef Medline](#)
- Lalitha P, Reddy M, Reddy KJ. **Extensive intracranial juvenile xanthogranulomas.** *AJNR Am J Neuroradiol* 2011;32:E132–33 [CrossRef Medline](#)
- Patrizi A, Neri I, Bianchi F, et al. **Langerhans cell histiocytosis and juvenile xanthogranuloma: two case reports.** *Dermatology* 2004;209:57–61 [CrossRef Medline](#)
- Picarsic J, Pysker T, Zhou H, et al. **BRAF V600E mutation in juvenile xanthogranuloma family neoplasms of the central nervous system (CNS-JXG): a revised diagnostic algorithm to include pediatric Erdheim-Chester disease.** *Acta Neuropathol Commun* 2019;7:168 [CrossRef Medline](#)
- Ali MM, Gilliam AE, Ruben BS, et al. **Juvenile xanthogranuloma in Noonan syndrome.** *Am J Med Genet A* 2021;185:3048–52 [CrossRef Medline](#)
- Liy-Wong C, Mohammed J, Carleton A, et al. **The relationship between neurofibromatosis type 1, juvenile xanthogranuloma, and malignancy: a retrospective case-control study.** *J Am Acad Dermatol* 2017;76:1084–87 [CrossRef Medline](#)
- Cambiaghi S, Restano L, Caputo R. **Juvenile xanthogranuloma associated with neurofibromatosis 1: 14 patients without evidence of hematologic malignancies.** *Pediatr Dermatol* 2004;21:97–101 [CrossRef Medline](#)
- Zvulunov A, Barak Y, Metzker A. **Juvenile xanthogranuloma, neurofibromatosis, and juvenile chronic myelogenous leukemia; world statistical analysis.** *Arch Dermatol* 1995;131:904–08 [CrossRef Medline](#)
- Durham BH, Lopez Rodrigo E, Picarsic J, et al. **Activating mutations in CSF1R and additional receptor tyrosine kinases in histiocytic neoplasms.** *Nat Med* 2019;25:1839–42 [CrossRef Medline](#)
- Ginat DT, Vargas SO, Silvera VM, et al. **Imaging features of juvenile xanthogranuloma of the pediatric head and neck.** *AJNR Am J Neuroradiol* 2016;37:910–16 [CrossRef Medline](#)
- Dehner LP. **Juvenile xanthogranulomas in the first two decades of life: a clinicopathologic study of 174 cases with cutaneous and extracutaneous manifestations.** *Am J Surg Pathol* 2003;27:579–93 [CrossRef Medline](#)
- Prosch H, Grois N, Wnorowski M, et al. **Long-term MR imaging course of neurodegenerative Langerhans cell histiocytosis.** *AJNR Am J Neuroradiol* 2007;28:1022–28 [CrossRef Medline](#)
- Prayer D, Grois N, Prosch H, et al. **MR imaging presentation of intracranial disease associated with Langerhans cell histiocytosis.** *AJNR Am J Neuroradiol* 2004;25:880–91 [Medline](#)
- Yeh EA, Greenberg J, Ablan O, et al; North American Consortium for Histiocytosis. **Evaluation and treatment of Langerhans cell histiocytosis patients with central nervous system abnormalities: current views and new vistas.** *Pediatr Blood Cancer* 2018;65:e26784 [CrossRef Medline](#)
- Boyd LC, O'Brien KJ, Ozkaya N, et al. **Neurological manifestations of Erdheim-Chester Disease.** *Ann Clin Transl Neurol* 2020;7:497–506 [CrossRef Medline](#)